



# Sea ice export through the Fram Strait derived from a combined model and satellite data set

Chao Min<sup>1,2,3</sup>, Longjiang Mu<sup>4</sup>, Qinghua Yang<sup>1,2,3</sup>, Robert Ricker<sup>4</sup>, Qian Shi<sup>1,3</sup>, Bo Han<sup>1,3</sup>, Renhao Wu<sup>1,3</sup>, Jiping Liu<sup>5</sup>

5 <sup>1</sup>School of Atmospheric Sciences and Guangdong Province Key Laboratory for Climate Change and Natural Disaster Studies, Sun Yat-sen University, Zhuhai, 519082, China

<sup>2</sup>State Key Laboratory of Numerical Modeling for Atmospheric Sciences and Geophysical Fluid Dynamics, Institute of Atmospheric Physics, Chinese Academy of Sciences, Beijing, 100029, China

<sup>3</sup>Southern Marine Science and Engineering Guangdong Laboratory (Zhuhai), Zhuhai, 519082, China

10 <sup>4</sup>Alfred Wegener Institute, Helmholtz Centre for Polar and Marine Research, Bremerhaven, 27570, Germany

<sup>5</sup> Department of Atmospheric and Environmental Sciences, University at Albany, State University of New York, New York, 12222, US

*Correspondence to:* Longjiang Mu (longjiang.mu@awi.de)

**Abstract.** Sea ice volume export through the Fram Strait plays an important role on the Arctic freshwater and energy  
15 redistribution. The combined model and satellite thickness (CMST) data set assimilates CryoSat-2 and Soil Moisture and Ocean Salinity (SMOS) thickness products together with satellite sea ice concentration. The CMST data set closes the gap of stand-alone satellite-derived sea ice thickness in summer and therefore allows us to estimate sea ice volume export during the melt season. In this study, we first validate the CMST data set using field observations, and then estimate the continuous seasonal and interannual variations of Arctic sea ice volume flux through the Fram Strait from September 2010 to December  
20 2016. The results show that seasonal and interannual sea ice volume export vary from -244 ( $\pm 43$ ) to -973 ( $\pm 59$ ) km<sup>3</sup> and -1974 ( $\pm 291$ ) to -2491 ( $\pm 280$ ) km<sup>3</sup>, respectively. The sea ice volume export reaches its maximum in spring and the mean amount of the melt season ice volume export accounts about one third of the yearly total amount. The minimum monthly sea ice export is -11 km<sup>3</sup> in August 2015 and the maximum (-442 km<sup>3</sup>) appears in March 2011. Seasonal variations of sea ice thickness and drift frequency distributions infer that the thicker ice accompanied with slower ice motion is more easier to appear when there  
25 is sea ice exporting through the Fram Strait outlet in summer.

## 1 Introduction

The sea ice extent and volume in the Arctic region that are sensitive to global climate change are persistently undergoing a decline for the past several decades and will likely continue to decrease since the start of 21st century (Comiso and Hall, 2014; Meier et al., 2014; Stroeve and Notz, 2015). The decline of ice extent changes the surface albedo, and as a consequence, the  
30 absorption of solar shortwave radiation increases. The variability of ice volume, however, exerts influence on heat, freshwater budget and weather systems in the lower latitudes (Gregory et al., 2002; Tilling et al., 2015). Correspondingly, both the thermodynamic processes and dynamic processes can impact Arctic sea ice mass budget. Generally, the sea ice outflow driven



by atmospheric circulation is an important component of dynamic processes. The Fram Strait serves as the primary outlet of the Arctic sea ice export (Krumpen et al., 2016). Moreover, the ice outflow through the strait into the Nordic Seas covers approximately 25% of the total Arctic freshwater export (Lique et al., 2009; Serreze et al., 2006).

Variations of satellite-based Arctic sea ice volume and sea ice export through the Fram Strait have been estimated by numerous studies (Bi et al., 2018; Kwok and Cunningham, 2015; Ricker et al., 2018; Ricker et al., 2017; Spreen et al., 2009). Nevertheless, with respect to the volume flux, the primary focus of these studies are the variations during the winter season (October–April). This is mainly due to the limitations in retrieving sea ice thickness and motion by satellite remote sensing during the melt season (May–September). It is mainly caused by more melt ponds and saturated water vapor in the sea ice surface, which restrains satellite-based ice thickness limited to the cold season only (Mu et al., 2018a). The speed-up of sea ice drift usually accompanies with thin summer sea ice, meanwhile the faster sea ice drifts the larger retrieving errors there would be (Spreen et al., 2011; Sumata et al., 2014). Melting sea ice with a less scattering surface could significantly suppress the signal-to-noise ratio and obstruct the employment of satellite imagery to retrieve ice drift. For above-mentioned reasons, the spaceborne sea ice drift data usually induce much more uncertainties in the melt season. All these deficiencies make the estimate of the Arctic sea ice thickness and drift variation all year round difficult with only satellite sea ice data.

Sea ice volume flux, compared to area flux, could reflect the sea ice mass balance in a more comprehensive way. However, the amounts of Fram strait sea ice volume export during the winter season do not demonstrate a conspicuous growth or decline trend (Ricker et al., 2018; Spreen et al., 2009). And the variation of the melt season ice volume flux through the Fram Strait still remains a query owing to the fact that sea ice thickness observations are sparse in the melt season, and so does the yearly total amount of ice volume flux. In terms of sea ice volume flux, Ricker et al. (2018) and Bi et al. (2018) point out that the variation of ice drift plays the major role in determining the annual and interannual ice volume export variability. Due to thermodynamic growth and deformation, the sea ice thickness on the other hand drives the increase in the seasonal cycle of exported volume. For this reason, an accurate data set of sea ice drift and thickness is crucial to better estimate sea ice volume output. However, the limitations of spaceborne sea ice thickness and drift data during the melt season poses a great challenge to derive the sea ice flux.

Employing the benefits of both the CryoSat-2 (CS2) and the Soil Moisture and ocean Salinity satellite (SMOS) sea ice thickness products, the new data set (combined model and satellite thickness, CMST) that assimilates these data together with satellite-derived sea ice concentration (Mu et al., 2018a; Mu et al., 2018b) provides the daily sea ice thickness, concentration and drift estimates simultaneously. Moreover, taking advantages of model dynamics and sea ice concentration assimilation, the new sea ice data set extends to cover the melt season when satellite data are limited (Mu et al., 2018a). Previous results reveal that CMST data even have some advantages among the statistically merged satellite data CS2SMOS and Pan-Arctic Ice-Ocean Modeling and Assimilation System (PIOMAS) thickness product when comparing with the in-situ observations (Mu et al., 2018a). Therefore, the CMST sea ice product enables to examine the all-year-round changes in sea ice volume export through the Fram Strait for 2010–2016, during a time when Arctic sea ice is undergoing dramatic changes. Further, we also calculate the sea ice thickness, concentration and drift frequency distributions along the main sea ice export gate all-year-round.



This paper is organized as follows. Section 2 describes the data used to derive volume flux and validate the CMST data, including CMST data set, OSISAF and NSIDC sea ice drift data, HEM sea ice thickness and ULS thickness. In section 3, firstly, we evaluate the performance of CMST data. Then, we estimate the continuous seasonal and interannual variation of sea ice thickness, concentration and drift in the Fram Strait. Also, the all-year-round variability of sea ice volume export through the Fram Strait is calculated. Uncertainty in our volume flux estimate is discussed in Section 4. Concluding remarks are given in Section 5.

## 2 Data and Methods

### 2.1 CMST sea ice data

75 The new CMST estimation data are generated by an Arctic regional ice-ocean model accompanying with CS2, SMOS sea ice thickness and SSMIS sea ice concentration assimilated. This Arctic regional model (Losch et al., 2010; Mu et al., 2017; Nguyen et al., 2011; Yang et al., 2014) is configured on the basis of the Massachusetts Institute of Technology generation circulation model (MITgcm) (Marshall et al., 1997). To reflect the impacts of atmospheric uncertainties on the sea ice data assimilation, the atmospheric ensemble forecasts of the United Kingdom Met Office (UKMO) Ensemble Prediction System (EPS; 80 <http://tigge.ecmwf.int>) are used as atmospheric forcing (Mu et al., 2018b; Yang et al., 2015; Yang et al., 2016). The Parallel Data Assimilation Framework (PDAF) is applied to assimilate satellite thickness (e.g., SMOS thickness data thinner than 1 m and weekly mean CS2 thickness data) and concentration data (provided by the Integrated Climate Data Center, <http://icdc.cen.uni-hamburg.de>). More details about this assimilation process can be found in previous studies (Mu et al., 2018a; Mu et al., 2018b). CMST provides grid cell-averaged ice thickness, i.e., the effective ice thickness (Mu et al., 2018a; 85 Schweiger et al., 2011) with a resolution about 18 km. Further taking advantage of model dynamics and ice concentration assimilation, the daily CMST thickness data in summer are also available from October 2010 to December 2016. Although the time span of CMST data do not contain the recent two years (e.g., year of 2017 and 2018), it does cover the year of the lowest sea ice extent record at that time (e.g., 2012 and 2016) (Parkinson and Comiso, 2013; Petty et al., 2018).

### 2.2 OSI SAF drift data

90 As suggested by Sumata et al. (2014), the merged OSI SAF sea ice drift product (OSI-405) reveals a better performance than other sea ice drift data sets in the Fram Strait. Thus, we use it for comparison with CMST drift data when calculating sea ice volume export. The merged drift data can be downloaded from the Ocean and Sea Ice Satellite Application Facility (OSI SAF, <http://www.osi-saf.org/?q=content/sea-ice-products>). The merged drift products are retrieved from multiple sensors and channels (shown in Table 1) in order to supplement data gaps in the single-sensor products. A more detailed description can 95 be seen in the Low Resolution Sea ice Drift Product User's Manual ([http://osisaf.met.no/p/ice/lr\\_ice\\_drift.html](http://osisaf.met.no/p/ice/lr_ice_drift.html)).



### 2.3 NSIDC sea ice drift

The latest released Polar Pathfinder Daily 25 km EASE-Grid sea ice drift data from the National Snow and Ice Data Center (NSIDC, <https://nsidc.org/data/nsidc-0116/versions/4>) are used to evaluate the CMST drift too. These data cover both the melt season and the freezing season and widely used in the modeling and data assimilation (Miller et al., 2006; Stark et al., 2008).

100 The input sea ice motion data sets are obtained from AVHRR, AMSR-E, SMMR, SSM/I, SSM/I, International Arctic Buoy Program (IABP) buoys and National Center for Environmental Prediction (NCEP) / National Center for Atmospheric Research (NCAR) Reanalysis wind data. More descriptions can be seen in the NSIDC ice motion user guide (<https://nsidc.org/data/nsidc-0116/versions/4>).

### 2.4 HEM sea ice thickness

105 For the purpose of evaluating the performance of CMST sea ice thickness, the helicopter-borne electromagnetic induction sounding (HEM) sea ice thickness (<https://www.nordatanet.no/en>) is utilized for intercomparison. This HEM measurement campaigns consist of 9 separate flights implemented in the Fram Strait from August to September, 2014. The helicopter-measured sea ice thickness is named as “total thickness” including snow layer. Thus, following Krumpfen et al. (2016), we assume the thickness of snow or weathered ice is 0.1 m, i.e., we subtract the 0.1 m snow thickness from the “total thickness”  
110 in the later calculation. Sea ice concentration is low in the operational areas during this period and the data have not been adjusted with sea ice concentration. Because the CMST model thickness are effective thickness (e.g., mean thickness over one model grid), for easy comparison, and as recommended by the data providers (<https://www.nordatanet.no/en>), we adjust this data with the CMST ice concentration to obtain daily mean ice thickness.

### 2.5 ULS sea ice thickness

115 The upward looking sonars (ULS) measurement (moored at 79°N, 5°W) in the Fram Strait is deployed and maintained by the Norwegian Polar Institute. The sea ice thickness derived from the ULS is rarely obscured by the snow layer depth and ice density errors. So the ULS observed sea ice thickness is further used to validate the CMST thickness. More details about the ULS data can be found in previous work (Hansen et al., 2013). In this study, only a one-year-round (from September, 2010 to August, 2011) monthly mean ULS sea ice thickness is used owing to the limited availability of this in-situ observations.

### 120 2.6 Retrieving methods in sea ice volume export

The sea ice thickness, concentration and drift in CMST data set are provided on the cube spherical Arakawa C grid with a resolution of 18 km. Both sea ice variables in CMST and the OSI-405 merged data are projected to the geographic coordinates at first. Following Krumpfen et al. (2016) and Ricker et al. (2018), we define the Fram Strait export gate with zonal and meridional components as shown in Figure 1. The zonal gate is situated at 82°N between 12°W and 20°E, and the meridional  
125 gate is located at 20°E between 80.5°N and 82°N. The chosen gates are dedicated to decrease errors and bias in low resolution



drift data and thickness data from satellite (Krumpfen et al., 2016; Ricker et al., 2018). Secondly, we interpolate the CMST data and OSI SAF data onto the zonal gate with a spatial resolution of  $1^\circ$  and the meridional gate with a spatial resolution of  $0.15^\circ$ , which is of the purpose to better match the model grids with the interpolated grids.

Following Ricker et al. (2018), the sea ice volume flux can be estimated as following formulas:

$$130 \quad Q_x = L_x H_x v, \quad (1)$$

$$Q_y = L_y H_y u, \quad (2)$$

where  $L_x$  is the size of zonal interpolated grid while  $L_y$  is the size of meridional interpolated grid.  $H_x$  and  $v$  are the interpolated effective ice thickness and velocity at the zonal gate.  $H_y$  and  $u$  are the interpolated effective ice thickness and velocity at the meridional gate. Note that ice concentration information is not involved in equations (1) and (2) because the calculation process of CMST model effective ice thickness has already taken ice concentration information into account.

135

The total sea ice volume export ( $Q_{EX}$ ) through the Fram Strait is obtained by adding the zonal ice volume flux ( $Q_x$ ) and meridional ice flux ( $Q_y$ ) together:

$$Q_{EX} = Q_x + Q_y, \quad (3)$$

Uncertainties of sea ice volume export ( $\delta_{Q_x}$ ) are evaluated as:

$$140 \quad \delta_{Q_x} = L_x \sqrt{(H \delta_v)^2 + (v \delta_H)^2}, \quad (4)$$

This strategy is used to estimate the expected uncertainties of volume flux via the zonal gate.  $\delta_v$  and  $\delta_H$  represent ice drift uncertainty and ice thickness uncertainties, respectively. Expected sea ice volume flux uncertainties along the meridional gate can be determined by the similar method of (4).

Detailed sea ice volume export derived from CMST thickness and drift are represented by M2 in Table 2 (Section 3.2). The results derived from CS2 thickness and OSI SAF drift for Ricker et al. (2018) are represented by R. To investigate the flux biases due to the existing deviations between the CMST and the CS2 thickness data, ice thickness from CMST and ice drift from OSI SAF are also used to calculate the flux that is also shown by M1.

145

### 3 Results

#### 3.1 validation of CMST data

150 Firstly, the field observations are used to evaluate the performance of CMST sea ice data in the Fram Strait. Comparing the mean sea ice drift of nearly 6 years' CMST data (shown in Figure 1a) with the latest released sea ice drift data (V4) from the NSIDC (shown in Figure 1b), we find that the circulation patterns (the Transport Drift and the Beaufort Gyre) and magnitudes of these two sea ice drift data (CMST vs. NSIDC) are both quite similar. The relatively large difference of sea ice velocity



magnitudes occurs in the southwestern Greenland Sea along the coast of Greenland. The mean sea ice thickness is distributed  
155 as expected and within the current understanding (Figure 1a). Further assessments of CMST thickness and drift data are shown  
in Figure 2. The geography map (Figure 2a) shows the trajectories of HEM measurement campaigns and the site of ULS.  
Helicopter-borne daily mean sea-ice thickness is first used to evaluate the CMST thickness data in the Fram Strait in this study.  
Monthly CMST sea ice thickness is also compared with the thickness derived from the ULS data (shown in Figure 2c). Note  
that the comparison period for CMST thickness and ULS thickness is from September 2010 to August 2011, since the ULS  
160 data afterwards have not been available for this study. Monthly CMST sea ice drift over the entire Fram Strait is evaluated  
with OSI SAF (from Ricker et al. 2018 for comparison) product. For quantitative metrics, correlation coefficient (CC), relative  
bias (RB) and root-mean-squared error (RMSE) are explored to quantify the comparison. These statistic metrics are calculated  
as follows (Chen et al., 2013; Zhang et al., 2019):

$$CC = \frac{\text{Cov}(\text{CMST}, \text{observation})}{\sigma_{\text{CMST}} \sigma_{\text{observation}}}, \quad (5)$$

$$165 \quad RB = \frac{\sum (\text{CMST} - \text{observation})}{\sum \text{observation}}, \quad (6)$$

$$RMSE = \sqrt{\frac{(\text{CMST} - \text{observation})^2}{N}}, \quad (7)$$

Statistical analysis between CMST and HEM sea ice thickness shows that the CC, RB and RMSE are 0.59, 15.13% and 0.66  
m, respectively. Furthermore, statistics indicate that the CMST data is comparable to ULS measurements with a CC of 0.68, a  
low RB (1.74%) and RMSE (0.328 m). Note that the CMST thickness has been already quantitatively evaluated with more  
170 observation records by a previous study (Mu et al., 2018a) and exhibits some advantages over the widely used CS2SMOS and  
PIOMAS thickness data. The CC between CMST drift and OSI SAF drift shows a high correlation of 0.93 (Figure 2d) in the  
freezing season (October-April). The RB (-6.05%) and RMSE (0.985 km d<sup>-1</sup>) are also relatively quite low. These statistical  
metrics suggest a good performance of CMST over the Fram Strait outlet in simulating the real sea ice drift and thickness.

### 3.2 Sea ice thickness, concentration and drift variation

175 For convenience, so we define the spring (March-May), summer (June-August), autumn (September-November) and winter  
(December-February) periods, respectively. The continuous and all-year-round covered seasonal variation of Arctic sea ice  
thickness and concentration are shown in Figures 3 and 4. During the study period, both the Arctic sea ice thickness and  
concentration show a significant seasonal variation, e.g., the sea ice thickness reach its maximum in spring (except for 2013),  
while the sea ice concentration has a peak value in spring/winter.

180 As shown in Figure 3, the distribution of sea ice thickness along the Fram Strait zonal gate features thicker sea ice in the east  
of Greenland than that in the west of Svalbard, showing a gradually thinning trend from west to east. Along with the meridional  
gate, sea ice is thickening from the northern Svalbard to the central Arctic Ocean. Note that the sea ice thickness hits its  
minimum in the autumn of 2011, and such anomaly is also found in previous studies based on sea ice satellite data (Kwok and





185 Cunningham, 2015; Tilling et al., 2015). Also, it is notable that the mean thickness of the winter 2013 arises a significant thickening comparing with other winters. This remarkable thickening may be linked to the anomalously cooling in 2013 which enhances the thermodynamic ice growth (Tilling et al., 2015).

Further analysis on the Arctic sea ice volume (inside the Arctic circle) shows a typical seasonal and interannual variations with the minimum in autumn and the maximum in spring. The Arctic sea ice volume undergoes a minimum season in the autumn of 2011 ( $6.93 \times 10^3 \text{ km}^3$ ) and reaches a maximum of  $20.19 \times 10^3 \text{ km}^3$  in the spring of 2014. The connection between the emerging  
190 time of maximum/minimum sea ice volume and extent is not particularly strong, for instance, the sea ice extent minimum ( $5.17 \times 10^6 \text{ km}^2$ ) happens in autumn of 2012 and the maximum of  $10.87 \times 10^6 \text{ km}^2$  occurs in spring of 2013 while the sea ice volume minimum ( $6.93 \times 10^3 \text{ km}^3$ ) happens in autumn of 2011 and the maximum of  $20.19 \times 10^3 \text{ km}^3$  occurs in spring of 2014. The temporal variation trends of Arctic ice volume and extent are similar to the results from Tilling et al. (2015) and Kwok and Cunningham (2018).

195 The sea ice thickness, concentration and drift averaged over the entire Fram Strait gate are shown in Figures 5, 6 and 7, respectively. We also compare these sea ice variables with Ricker et al. (2018). The results show that the CMST ice thickness and drift are slightly smaller than that of CS2 and OSI SAF while the CMST ice concentration is a little larger than OSI SAF ice concentration. The underestimation of sea ice thickness in the Fram Strait is reasonable (Figure 6 in Mu et al., 2018b). The previous study shows that the mean Arctic-wide OSI SAF drift is slightly larger than IABP/D buoy ice drift (Sumata et al.,  
200 2014), which suggests the slight underestimation of CMST drift seems also tenable. Further validation with more ice drift data (e.g., high resolution SAR drift data and buoy drift data) is needed; however, it is beyond the scope of this work. In terms of variation trend, they are in good agreement with those of Ricker et al. (2018). As shown in Figures 5 and 7, the averaged sea ice thickness and drift reveal a significant seasonal cycle. That is, the variations of sea ice thickness and motion always accompany with spring augment and autumn decrease. The analysis of ice concentration shows a moderate decline in the melt  
205 season. And the 6-year mean sea ice thickness, concentration and drift averaged over the entire Fram Strait gate are about 1.7 m, 85% and  $5 \text{ km d}^{-1}$ .

Following Ricker et al. (2018), the relative standard deviation ( $\text{RSD} = \text{SD}/\text{mean}$ ) is used to measure the effects of sea ice variables on volume output. Variables with a larger RSD contributes to a greater impact on the volume variation. As shown in Figures 5, 6 and 7, the RSD of ice thickness is 0.30 which is about twice of ice concentration (0.14). The RSD of ice drift is  
210 0.50 which is the largest contributor. Consistent with previous studies, such as Ricker et al. (2018) and Bi et al. (2018), the ice drift with maximal RSD is more likely to affect variations in sea ice volume flux.

For further analysis of the impacts on the seasonal variations of sea ice volume flux, we present the seasonal sea ice thickness (Figure 8), drift (Figure 9) and concentration (not shown owing to the minimum RSD) frequency distributions along the Fram Strait outlet. As suggested by Figure 8, the thickness along the zonal gate is much thicker than the meridional gate. The mean  
215 fraction (approximately 73% of zonal gate) of summer sea ice thickness thicker than 2 m is larger than other seasons during the study period (except the summer of 2011). Nevertheless, the mean relative frequency of sea ice drift distribution (Figure 9) shows that the ratio of summer sea ice drift lower than  $6 \text{ km d}^{-1}$  is in the majority (approximately 93% of zonal gate),



220 indicating that the sea ice drift is much slower than other seasons. Also, the ice drift along the zonal gate is usually faster than the meridional gate. And it can be found that the spring and winter ice concentration along the zonal gate is larger than that of summer and autumn.

### 3.3 Sea ice volume export through the Fram Strait

225 In this section, sea ice volume export over all seasons is investigated. Firstly, the examination of monthly Arctic sea ice volume export through the Fram Strait is demonstrated in Table 2. Both our results and Ricker et al. (2018) find that the maximum monthly sea ice export takes place in March 2011. The maximum of CMST data is  $-442 \text{ km}^3$  (notice that the negative values represent ice volume loss from the Arctic Basin through the outlet) that is less than that ( $-540 \text{ km}^3$ ) of Ricker et al. (2018). Consistently, the lowest sea ice output for each study occurs in February 2011 when excluding the melt season (May-September). The minimum of the results shown in Ricker et al. (2018) is  $-21 \text{ km}^3$  while that is  $-34 \text{ km}^3$  in CMST data. Although there are some differences in flux calculated based on CMST data and CryoSat-2 thickness and OSISAF drift data, both the estimations show a similar trend in annual cycle. Furthermore, the CMST data can provide sea ice variables (e.g., sea ice  
230 thickness, concentration and drift) in the melt season that remote sensing retrieval data cannot cover. Taking advantage of CMST data, this study is trying to fill the research gap in the summer sea ice volume export. It is found that another minimum of ice export occurs in August 2015 during the study period. The minimum value for CMST is  $-11 \text{ km}^3$  that is  $10 \text{ km}^3$  less than  $-21 \text{ km}^3$  (R) in February 2011 and  $23 \text{ km}^3$  less than that for M2.

235 Moreover, the seasonal variation of sea ice export through Fram Strait is shown in Figure 10. The ice volume output shows a significant seasonal variation. The seasonal maximums are found in spring of all years (2011-2016) and the low values usually occur in summer and autumn. The maximum seasonal ice export of  $-973 (\pm 59) \text{ km}^3$  takes place in the spring of 2012 owing to faster ice drift than other springs (shown in Figure 9), while the minimum flux of  $-244 (\pm 43) \text{ km}^3$  occurs in autumn of 2016 caused by rather slower ice motion than other autumns (shown in Figure 9). Unlike other autumn ice export, the ice volume export of autumn 2013 abnormally increases and reaches  $-621 (\pm 60) \text{ km}^3$ . This abnormal increase can be also explained by the  
240 faster ice drift (shown in Figure 9).

The CMST-based sea ice volume during both the melt season and the freezing season are first reported in this study. The estimations show that the mean ice volume export during the melt season is  $-751 (\pm 117) \text{ km}^3$  which is about half of that during the freezing season ( $1503 \pm 158 \text{ km}^3$ ). Annually, sea ice volume export (Figure 11) is also calculated and varies from  $-1974 (\pm 291)$  to  $-2491 (\pm 280) \text{ km}^3$ . It is verified again that the annual sea ice volume export through the Fram Strait does not show a  
245 significant growth or decline trend (Ricker et al., 2018; Spreen et al., 2009). And the minimum yearly ice volume export occurs in the year of 2013 while the ice volume export reaches its maximum in 2012. This decline in ice volume export derives from both mean thickness and drift speed drop through the Fram Strait.





#### 4 Discussions

The ensemble standard deviation (SD) map of CMST ice concentration, thickness and drift shows that uncertainties are larger downstream the east of Greenland (Figures 12). So, following Krumpfen et al. (2016) and Ricker et al. (2018), a different gateway over the Fram Strait that consists of a zonal gate and a meridional gate located at a slightly higher latitude comparing to previous studies is chosen (Kwok et al., 2004; Kwok and Rothrock, 1999; Spreen et al., 2009). Alternatively, the choice of lower latitude gate at 79°N (e.g., the ULS moored sites) is suggested to utilize the ULS thickness for rough volume flux calculation when ice thickness data is unavailable. It should be noted that the different locations of Fram Strait gate and study period will introduce deviations on ice volume estimation (Krumpfen et al., 2016; Kwok et al., 2004; Kwok and Rothrock, 1999; Mu et al., 2017; Ricker et al., 2018; Spreen et al., 2009). The bottom melting and underestimation of sea ice motion will result in lower estimation of ice volume flux if a lower latitude gate is used (Spreen et al., 2009; Wekerle et al., 2017). For example, Ricker et al. (2018) investigated the sea ice flux in the Fram Strait and pointed out that the maximum (-540 km<sup>3</sup>) occurs in March of 2011 and the minimum (-21 km<sup>3</sup>) appears in February of 2011 from 2010 to 2017. However, on the different gate and period, Spreen et al. (2009) showed a relatively low maximum volume export of -420 km<sup>3</sup> and relatively high minimum flux (-92 km<sup>3</sup>) in the freezing season.

We investigate the similar period with Ricker et al. (2018), but further extend the sea ice volume flux estimation to include the summer seasons. Also, the CMST sea ice thickness data used in this study are evaluated to be reasonable when compared with in-situ observations (Mu et al., 2018a). The other important driver (sea ice drift) of ice volume export has also been compared with OSI SAF drift used in former estimations (Ricker et al., 2018). The monthly mean ice drift of CMST and OSI SAF shows a good consistency (Figure 2d and Figure 7). Furthermore, the CMST ice drift can provide the absent values where remote sensing data cannot detect. The estimation of volume export in this study reveals a reasonable sea ice volume export all year round.

The nearly 6 years' ice volume export through the Fram Strait is calculated and shown in Table 2. Besides the ice volume export (R) of Ricker et al. (2018), we also calculate the export using OSI SAF drift and CMST thickness (M1) and CMST thickness and drift (M2), respectively. It can be concluded that R is larger than M1 and M2 because R is derived from thicker CS2 thickness (Figure 5) and relatively faster OSI SAF drift (Figure 7). In addition, M1 is generally larger than M2 due to the faster ice motion for most periods. M2 is sometimes larger than M1 owing to the larger CMST ice motion than that of OSI SAF. For example, there are five months of M2 in the freezing season of 2014 that are larger than M1. One reason is that both M1 and M2 are based on the same CMST thickness but the CMST sea ice drift is faster than OSI SAF in the months of March, April and November.

We have calculated the ice export in the zonal gate and the meridional gate covering both the melt season and the freezing season, respectively. The ice volume export through the meridional outlet shows a more robust increase from autumn to spring while the annual mean meridional ice export is only 8% of zonal gate (shown in Figure 10). To further validate the sea ice volume export in the melt season, we compare our CMST-based volume flux (e.g., M2) with the relative short-term summer



ice volume flux that Krumpfen et al. (2016) derived from airborne ice thickness and NSIDC ice drift data. The intercomparison shows that the sea ice volume export in August 2011 and July 2012 estimated by Krumpfen et al. (2016) are smaller than this study. The underestimation of summer sea ice volume may deduce from a general underestimation of NSIDC drift during the melt season (Krumpfen et al., 2016; Sumata et al., 2015; Sumata et al., 2014). Additionally, Kwok et al. (1999 and 2004) investigated the summer sea ice export by using ULS thickness and area flux in the freezing season. The average annual ice volume flux is  $2218 \text{ km}^3 \text{ yr}^{-1}$  from 1991 to 1998 while the mean sea ice volume export from 1990 to 1995 is  $2366 \text{ km}^3 \text{ yr}^{-1}$  (Kwok et al., 2004; Kwok and Rothrock, 1999). The annual average volume flux in this study is  $2254 \text{ km}^3 \text{ yr}^{-1}$  that is similar to the volume flux from 1991 to 1998 (Kwok et al., 2004) and a little smaller than the period of 1990-1995 (Kwok and Rothrock, 1999). In a recent study (Wei et al., 2019), Wei et al. (2019) calculates the annual mean sea ice volume export ( $3216 \text{ km}^3 \text{ yr}^{-1}$ ) through the Fram Strait using MITgcm-ECCO2 during 1979 to 2012. Their estimations give a long period of sea ice volume export through the Fram Strait which can serve as an important reference when focusing on the long-term trend and variation of volume flux. However, this estimation derived from MITgcm-ECCO2 seems to overestimate the volume flux owing to the overestimations of sea ice drift and thickness (Wei et al., 2019). Therefore, the CMST data which assimilates CS2 and SMOS sea ice thickness and SSMIS sea ice concentration simultaneously have more advantages in calculating sea ice volume and extent export. Ricker et al. (2018) and Bi et al. (2018), gave their averaged freezing season volume export that are of  $1711 \text{ km}^3$  and  $1463 \text{ km}^3$ , respectively, based on the CS2 thickness data and different ice drift data over a similar period and outflow gates. Our average estimate of  $Q_{\text{EX,CMST,CMST}}$  (e.g., M2) based on the CMST ice thickness and drift is  $1575 \text{ km}^3$  while the  $Q_{\text{EX,CMST,OSISAF}}$  (e.g., M1) derived from CMST thickness and OSI SAF drift is  $1599 \text{ km}^3$  in the freezing season. The similar results between M1 and M2 are because that the CMST drift are comparable with OSI SAF drift in the cold seasons. But more reliable validations of CMST ice drift need more in-situ records and more systematic evaluations.

#### 4 Conclusions

The daily CMST data over all seasons are first used to estimate ice volume export through the Fram Strait. Also, benefitting from the advantage of CMST data, the melt season (e.g. summer season and autumn season) ice volume export can be derived to fill the data gap over such periods. The entire seasonal and interannual variations of Arctic sea ice volume are helpful for communities that focus on climate teleconnection between Polar regions and low latitudes, Arctic freshwater transport and ocean circulation. Conclusions of this study can be drawn as follows:

- (1) The Arctic sea ice thickness and volume show a significant seasonal variation. The thickness and volume maximum usually occur in spring and the Arctic sea ice volume hits its minimum in autumn 2011 during the study period.
- (2) Along the entire Fram Strait gate, the relative standard deviation (RSD) of ice drift (0.50) is greater than the RSD of ice thickness (0.30) and concentration (0.14), demonstrating that ice drift is a main driver of ice volume export through the Fram Strait.



(3) The mean sea ice volume export during the melt season is  $-751 (\pm 117) \text{ km}^3$  which is about 50% of that during the freezing season ( $1503 \pm 158 \text{ km}^3$ ). The lowest and largest annual sea ice volume export occur in 2013 and 2012, respectively. Seasonal sea ice volume export varies from  $-244 (\pm 43)$  to  $-973 (\pm 59) \text{ km}^3$  while the monthly sea ice export varies between  $-11 \text{ km}^3$  (August of 2015) and  $-442 \text{ km}^3$  (March of 2011) during this study period. The abnormal ice volume export increase in autumn 2013 is primarily associated with the faster ice motion.

(4) Seasonal variations of relative frequency of CMST sea ice thickness show that mean summer thickness thicker than 2 m (73% of zonal gate) through Fram Strait is more than other seasons (except the summer of 2011). The mean ratio of summer season ice drift (93% of zonal gate) lower than  $6 \text{ km d}^{-1}$  is in the majority. And the abnormal ice volume export increase in autumn 2013 is speculated to the faster ice motion.

The long-term series of sea ice volume export are more important for ocean-climate analysis. An updated and improved CMST V2 sea ice data will be developed in the near future, so that a longer ice volume exported estimations can be expected.

*Data availability.* The CMST sea ice data are available at <https://doi.pangaea.de/10.1594/PANGAEA.891475> (Mu et al., 2018, last access: 2 April 2019). The OSI SAF drift data can be download at <http://www.osi-saf.org/?q=content/sea-ice-products> (last access: 1 January 2019). The latest released Polar Pathfinder Daily 25 km EASE-Grid sea ice drift data are provided by the National Snow and Ice Data Center (NSIDC, <https://nsidc.org/data/nsidc-0116/versions/4>, last access: 2 May 2019). The helicopter-borne electromagnetic induction sounding (HEM) sea ice thickness are available at <https://www.nordatanet.no/en> (last access: 3 May 2019).

*Author contributions.* LM and QY conceptualized this study and provided the CMST sea ice data. CM conducted this study and performed the calculation. RR supplied the sea ice data of Ricker et al. (2018) for intercomparison. CM wrote this manuscript. LM, QY and RR polished this manuscript and improved the readability. QS, RW, BH and JL reviewed this manuscript.

*Competing interests.* The Authors declare that they have no conflict of interests.

*Acknowledgement.* This is a contribution to the Year of Polar Prediction (YOPP), a flagship activity of the Polar Prediction Project (PPP), initiated by the World Weather Research Programme (WWRP) of the World Meteorological Organization (WMO). Thanks are given to Yongwu Xiu, Ran Yang from School of Atmospheric Sciences, Sun Yat-sen University for the discussions. We also thank Yu Liang at Key laboratory of Marine Geology and Environment, Institute of Oceanology, Chinese Academy of Sciences for her advice and E. Hansen at Norwegian Polar Institute for providing the ULS data. This study is supported by National Key R&D Program of China (2018YFA0605901), the Opening fund of State Key Laboratory of Cryospheric Science (SKLCS-OP-2019-09), the Federal Ministry of Education and Research of Germany in the framework of SSIP (grant01LN1701A), and the National Natural Science Foundation of China (41776192, 41706224).



## References

- 340 Bi, H., Wang, Y., Zhang, W., Zhang, Z., Liang, Y., Zhang, Y., Hu, W., Fu, M., and Huang, H.: Recent satellite-derived sea ice volume flux through the Fram Strait: 2011–2015, *Acta Oceanol. Sin.*, 37, 107-115, doi:10.1007/s13131-018-1270-9, 2018.
- Chen, S., Gourley, J. J., Hong, Y., Kirstetter, P. E., Zhang, J., Howard, K., Flamig, Z. L., Hu, J., and Qi, Y.: Evaluation and Uncertainty Estimation of NOAA/NSSL Next-Generation National Mosaic Quantitative Precipitation Estimation Product (Q2) over the Continental United States, *J. Hydrometeorol.*, 14, 1308-1322, doi:10.1175/JHM-D-12-0150.1, 2013.
- 345 Comiso, J. C. and Hall, D. K.: Climate trends in the Arctic as observed from space, *WIREs. Clim. Change*, 5, 389-409, doi:10.1002/wcc.277, 2014.
- Gregory, J. M., Stott, P. A., Cresswell, D. J., Rayner, N. A., Gordon, C., and Sexton, D. M. H.: Recent and future changes in Arctic sea ice simulated by the HadCM3 AOGCM, *Geophys. Res. Lett.*, 29, 28-21-28-24, doi:10.1029/2001GL014575, 2002.
- Hansen, E., Gerland, S., Granskog, M. A., Pavlova, O., Renner, A. H. H., Haapala, J., Løyning, T. B., and Tschudi, M.: Thinning of Arctic sea ice observed in Fram Strait: 1990–2011, *J. Geophys. Res-Oceans.*, 118, 5202-5221, doi:10.1002/jgrc.20393, 2013.
- 350 Krumpen, T., Gerdes, R., Haas, C., Hendricks, S., Herber, A., Selyuzhenok, V., Smedsrud, L., and Spreen, G.: Recent summer sea ice thickness surveys in Fram Strait and associated ice volume fluxes, *The Cryosphere*, 10, 523-534, doi:10.5194/tc-10-523-2016, 2016.
- Kwok, R. and Cunningham, G. F.: Variability of Arctic sea ice thickness and volume from CryoSat-2, *Philos. T. R. Soc. A.*, 373, 20140157, doi:10.1098/rsta.2014.0157, 2015.
- 355 Kwok, R., Cunningham, G. F., and Pang, S. S.: Fram Strait sea ice outflow, *J. Geophys. Res-Oceans.*, 109, doi:10.1029/2003JC001785, 2004.
- Kwok, R. and Rothrock, D. A.: Variability of Fram Strait ice flux and North Atlantic Oscillation, *J. Geophys. Res-Oceans.*, 104, 5177-5189, doi:10.1029/1998JC900103, 1999.
- Lique, C., Treguier, A. M., Scheinert, M., and Penduff, T.: A model-based study of ice and freshwater transport variability along both sides of Greenland, *Clim. Dynam.*, 33, 685-705, doi: 10.1007/s00382-008-0510-7, 2009.
- 360 Losch, M., Menemenlis, D., Campin, J.-M., Heimbach, P., and Hill, C.: On the formulation of sea-ice models. Part 1: Effects of different solver implementations and parameterizations, *Ocean. Model.*, 33, 129-144, doi:10.1016/j.ocemod.2009.12.008, 2010.
- Marshall, J., Adcroft, A., Hill, C., Perelman, L., and Heisey, C.: A finite-volume, incompressible Navier Stokes model for studies of the ocean on parallel computers, *J. Geophys. Res-Oceans.*, 102, 5753-5766, doi:10.1029/96JC02775, 1997.
- 365 Meier, W. N., Hovelsrud, G. K., van Oort, B. E. H., Key, J. R., Kovacs, K. M., Michel, C., Haas, C., Granskog, M. A., Gerland, S., Perovich, D. K., Makshtas, A., and Reist, J. D.: Arctic sea ice in transformation: A review of recent observed changes and impacts on biology and human activity, *Rev. Geophys.*, 52, 185-217, doi:10.1002/2013RG000431, 2014.
- Miller, P. A., Laxon, S. W., Feltham, D. L., and Cresswell, D. J.: Optimization of a Sea Ice Model Using Basinwide Observations of Arctic Sea Ice Thickness, Extent, and Velocity, *J. Climate.*, 19, 1089-1108, doi:10.1175/JCLI3648.1, 2006.
- 370 Mu, L., Losch, M., Yang, Q., Ricker, R., Losa, S. N., and Nerger, L.: Arctic-Wide Sea Ice Thickness Estimates From Combining Satellite Remote Sensing Data and a Dynamic Ice-Ocean Model with Data Assimilation During the CryoSat-2 Period, *J. Geophys. Res-Oceans.*, 123, 7763-7780, doi:10.1029/2018JC014316, 2018a.
- Mu, L., Yang, Q., Losch, M., Losa, S. N., Ricker, R., Nerger, L., and Liang, X.: Improving sea ice thickness estimates by assimilating CryoSat-2 and SMOS sea ice thickness data simultaneously, *Q. J. Roy. Meteor. Soc.*, 144, 529-538, doi:10.1002/qj.3225, 2018b.



- 375 Mu, L., Zhao, J., and Zhong, W.: Regime shift of the dominant factor for halocline depth in the Canada Basin during 1990–2008, *Acta Oceanologica Sinica*, 36, 35-43, doi: 10.1007/s13131-016-0883-0, 2017.
- Nguyen, A. T., Menemenlis, D., and Kwok, R.: Arctic ice-ocean simulation with optimized model parameters: Approach and assessment, *J. Geophys. Res-Oceans*, 116, doi:10.1029/2010JC006573, 2011.
- Parkinson, C. L. and Comiso, J. C.: On the 2012 record low Arctic sea ice cover: Combined impact of preconditioning and an August storm,  
380 *Geophys. Res. Lett.*, 40, 1356-1361, doi:10.1002/grl.50349, 2013.
- Petty, A. A., Stroeve, J. C., Holland, P. R., Boisvert, L. N., Bliss, A. C., Kimura, N., and Meier, W. N.: The Arctic sea ice cover of 2016: a year of record-low highs and higher-than-expected lows, *The Cryosphere*, 12, 433-452, doi:10.5194/tc-12-433-2018, 2018.
- Ricker, R., Girard-Ardhuin, F., Krumpen, T., and Lique, C.: Satellite-derived sea ice export and its impact on Arctic ice mass balance, *The Cryosphere*, 12, 3017-3032, doi:10.5194/tc-12-3017-2018, 2018.
- 385 Ricker, R., Hendricks, S., Girard-Ardhuin, F., Kaleschke, L., Lique, C., Tian-Kunze, X., Nicolaus, M., and Krumpen, T.: Satellite-observed drop of Arctic sea ice growth in winter 2015–2016, *Geophys. Res. Lett.*, 44, 3236-3245, doi:10.1002/2016gl072244, 2017.
- Schweiger, A., Lindsay, R., Zhang, J., Steele, M., Stern, H., and Kwok, R.: Uncertainty in modeled Arctic sea ice volume, *J. Geophys. Res-Oceans.*, 116, doi:10.1029/2011JC007084, 2011.
- Serreze, M. C., Barrett, A. P., Slater, A. G., Woodgate, R. A., Aagaard, K., Lammers, R. B., Steele, M., Moritz, R., Meredith, M., and Lee,  
390 C. M.: The large-scale freshwater cycle of the Arctic, *J. Geophys. Res-Oceans.*, 111, doi:10.1029/2005JC003424, 2006.
- Spreen, G., Kern, S., Stammer, D., and Hansen, E.: Fram Strait sea ice volume export estimated between 2003 and 2008 from satellite data, *Geophys. Res. Lett.*, 36, doi:10.1029/2009gl039591, 2009.
- Spreen, G., Kwok, R., and Menemenlis, D.: Trends in Arctic sea ice drift and role of wind forcing: 1992–2009, *Geophys. Res. Lett.*, 38, doi:10.1029/2011GL048970, 2011.
- 395 Stark, J. D., Ridley, J., Martin, M., and Hines, A.: Sea ice concentration and motion assimilation in a sea ice–ocean model, *J. Geophys. Res-Oceans.*, 113, doi:10.1029/2007JC004224, 2008.
- Stroeve, J. and Notz, D.: Insights on past and future sea-ice evolution from combining observations and models, *Global Planet. Change.*, 135, 119-132, doi: 10.1016/j.gloplacha.2015.10.011, 2015.
- Sumata, H., Kwok, R., Gerdes, R., Kauker, F., and Karcher, M.: Uncertainty of Arctic summer ice drift assessed by high-resolution SAR  
400 data, *J. Geophys. Res-Oceans.*, 120, 5285-5301, doi:10.1002/2015JC010810, 2015.
- Sumata, H., Lavergne, T., Girard-Ardhuin, F., Kimura, N., Tschudi, M. A., Kauker, F., Karcher, M., and Gerdes, R.: An intercomparison of Arctic ice drift products to deduce uncertainty estimates, *J. Geophys. Res-Oceans.*, 119, 4887-4921, doi:10.1002/2013JC009724, 2014.
- Tilling, R. L., Ridout, A., Shepherd, A., and Wingham, D. J.: Increased Arctic sea ice volume after anomalously low melting in 2013, *Nat. Geosci.*, 8, 643, doi:10.1038/Ngeo2489, 2015.
- 405 Wei, J., Zhang, X., and Wang, Z.: Reexamination of Fram Strait sea ice export and its role in recently accelerated Arctic sea ice retreat, *Clim. Dyn.*, doi:10.1007/s00382-019-04741-0 2019.
- Wekerle, C., Wang, Q., Danilov, S., Schourup-Kristensen, V., von Appen, W.-J., and Jung, T.: Atlantic Water in the Nordic Seas: Locally eddy-permitting ocean simulation in a global setup, *J. Geophys. Res-Oceans.*, 122, 914-940, doi:10.1002/2016JC012121, 2017.
- Yang, Q., Losa, S., Losch, M., Tian-Kunze, X., Nerger, L., Liu, J., Kaleschke, L., and Zhang, Z.: Assimilating SMOS sea ice thickness into  
410 a coupled ice-ocean model, using a local SEIK filter, *J. Geophys. Res-Oceans.*, 119, 6680-6692, doi:10.1002/2014JC009963, 2014.
- Yang, Q., Losa, S. N., Losch, M., Jung, T., and Nerger, L.: The role of atmospheric uncertainty in Arctic summer sea ice data assimilation and prediction, *Q. J. Roy. Meteor. Soc.*, 141, 2314-2323, doi:10.1002/qj.2523, 2015.



- 415 Yang, Q., Losch, M., Losa, S. N., Jung, T., and Nerger, L.: Taking into Account Atmospheric Uncertainty Improves Sequential Assimilation  
of SMOS Sea Ice Thickness Data in an Ice–Ocean Model, *J. Atmos. Ocean. Tech.*, 33, 397-407, doi:10.1175/JTECH-D-15-0176.1, 2016.
- 420 Zhang, A., Xiao, L., Min, C., Chen, S., Kulie, M., Huang, C., and Liang, Z.: Evaluation of latest GPM-Era high-resolution satellite  
precipitation products during the May 2017 Guangdong extreme rainfall event, *Atmos. Res.*, 216, 76-85, doi:  
10.1016/j.atmosres.2018.09.018, 2019.

420

425

430

435

440

445





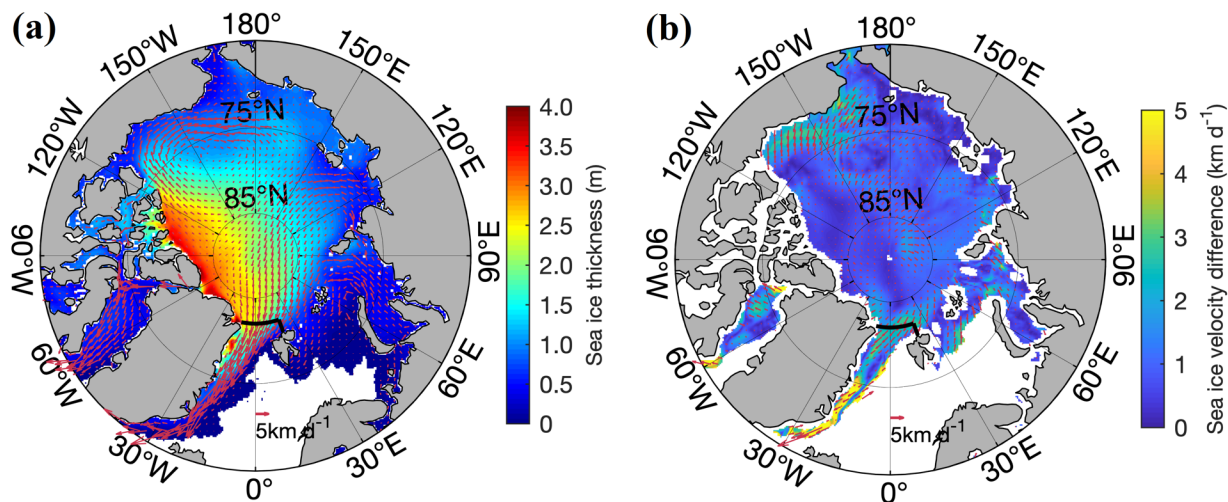
**Table 1.** OSI SAF drift data used in this study for comparison.

| Name    | Product          | Original data   | Algorithm | Temporal resolution | Spatial Resolution | Period    |
|---------|------------------|---|-----------|---------------------|--------------------|-----------|
| OSI SAF | OSI-405 (merged) | SSMIS (91 GHz, DMSP F17), ASCAT (Metop-B), AMSR-2 (18.7 and 37 GHz) | CMCC      | 2 days              | 62.5 km            | 2010-2016 |

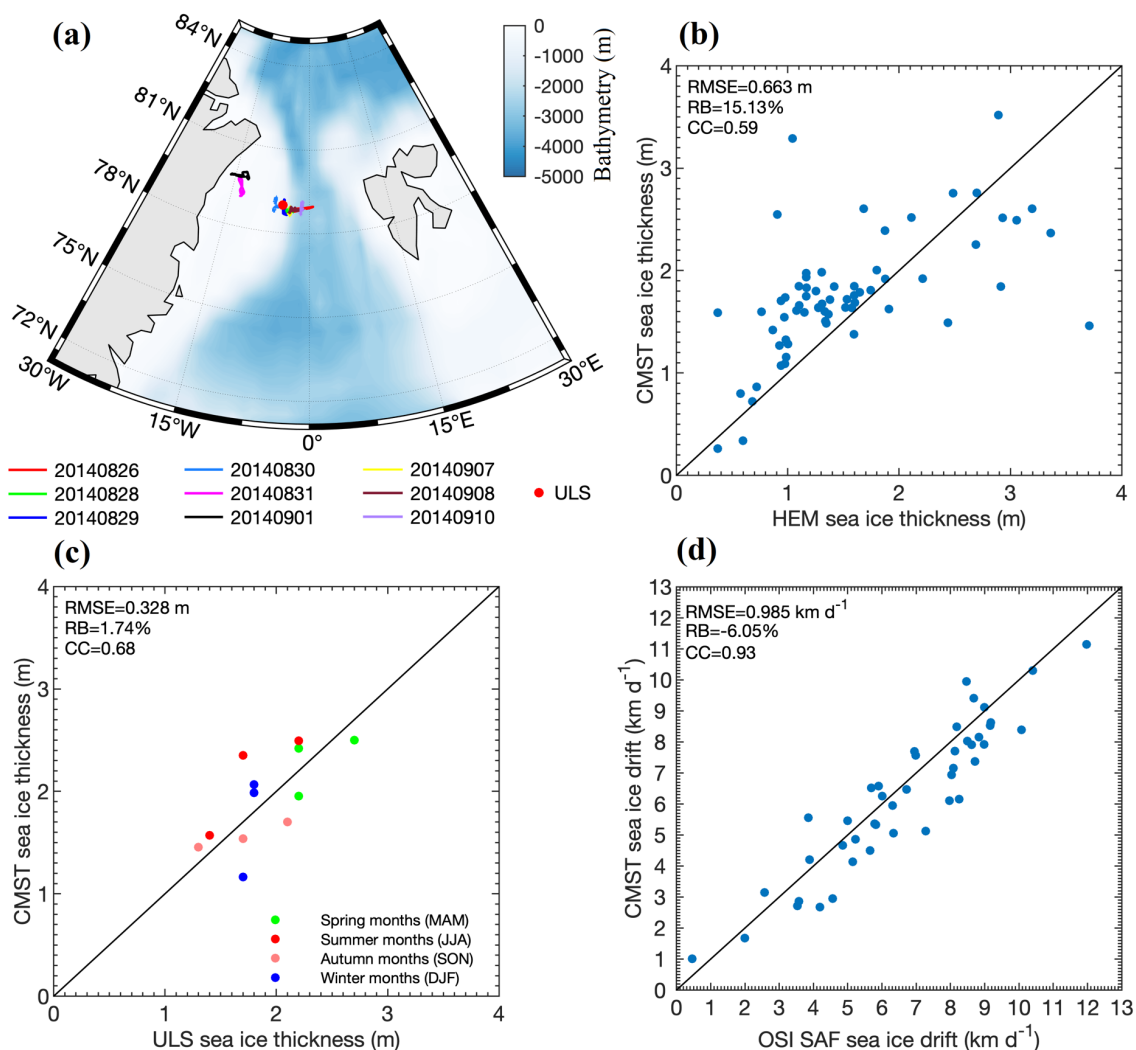
450

**Table 2.** Monthly Arctic sea ice volume export through the Fram Strait in km<sup>3</sup> month<sup>-1</sup>.

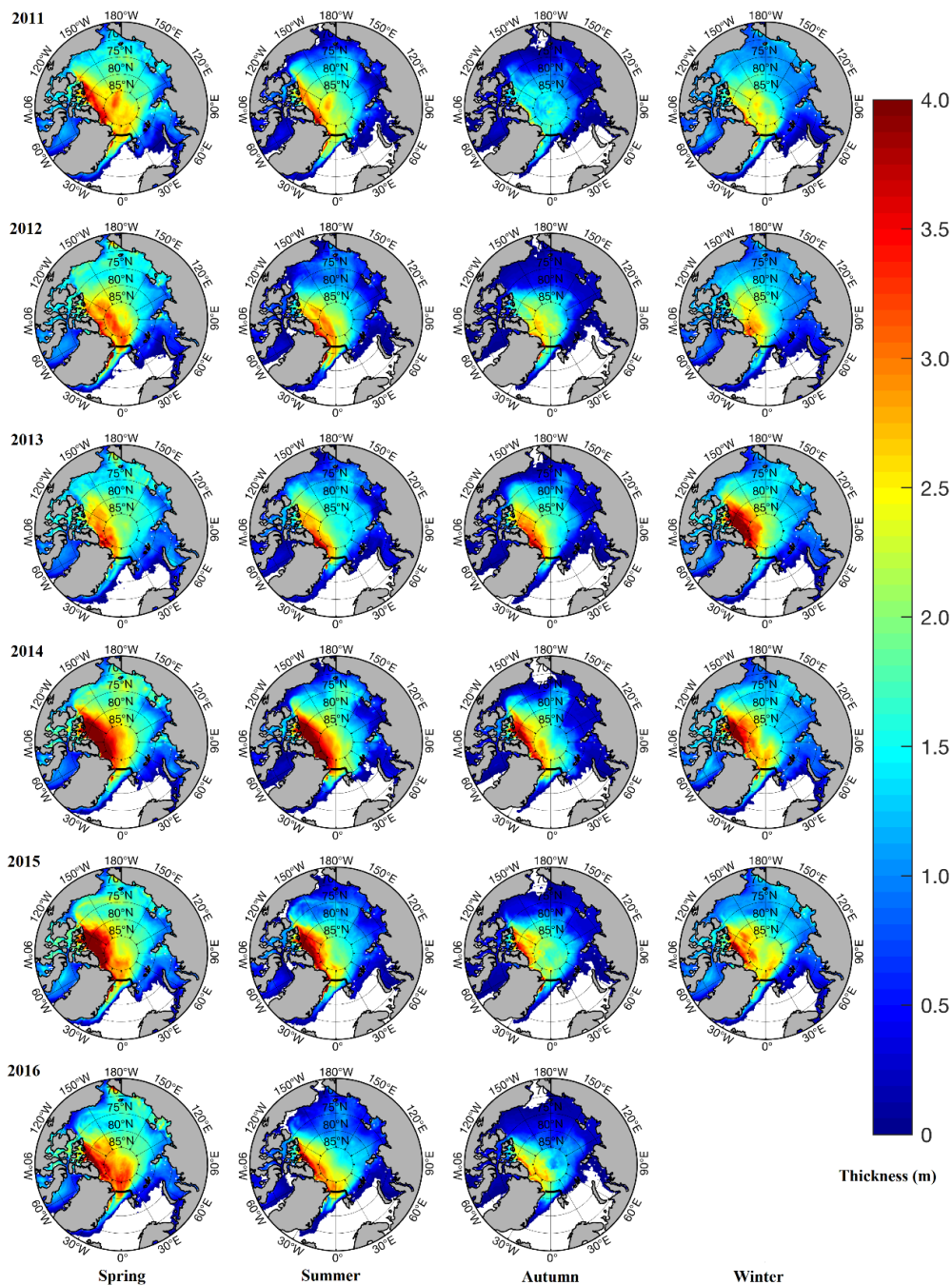
|      |    | Jan  | Feb        | Mar         | Apr  | May  | Jun  | Jul  | Aug        | Sep  | Oct  | Nov  | Dec  |
|------|----|------|------------|-------------|------|------|------|------|------------|------|------|------|------|
| 2010 | R  | —    | —          | —           | —    | —    | —    | —    | —          | —    | —    | -227 | -275 |
|      | M1 | —    | —          | —           | —    | —    | —    | —    | —          | —    | —    | -209 | -258 |
|      | M2 | —    | —          | —           | —    | —    | —    | —    | —          | -148 | -222 | -195 | -239 |
| 2011 | R  | -267 | <b>-21</b> | <b>-540</b> | -279 | —    | —    | —    | —          | —    | -164 | -214 | -354 |
|      | M1 | -238 | -24        | -478        | -255 | —    | —    | —    | —          | —    | -149 | -163 | -293 |
|      | M2 | -238 | -34        | <b>-442</b> | -230 | -278 | -185 | -115 | -64        | -28  | -151 | -175 | -290 |
| 2012 | R  | -129 | -381       | -379        | -487 | —    | —    | —    | —          | —    | -203 | -182 | -187 |
|      | M1 | -109 | -299       | -287        | -428 | —    | —    | —    | —          | —    | -207 | -157 | -125 |
|      | M2 | -137 | -300       | -267        | -372 | -334 | -218 | -187 | -131       | -100 | -160 | -149 | -136 |
| 2013 | R  | -103 | -163       | -299        | -318 | —    | —    | —    | —          | —    | -215 | -400 | -231 |
|      | M1 | -80  | -122       | -254        | -254 | —    | —    | —    | —          | —    | -212 | -372 | -211 |
|      | M2 | -78  | -109       | -217        | -219 | -194 | -140 | -107 | -98        | -26  | -228 | -367 | -191 |
| 2014 | R  | -78  | -195       | -345        | -452 | —    | —    | —    | —          | —    | -200 | -165 | -373 |
|      | M1 | -49  | -105       | -240        | -401 | —    | —    | —    | —          | —    | -203 | -122 | -307 |
|      | M2 | -61  | -114       | -282        | -425 | -232 | -161 | -112 | -184       | -194 | -170 | -162 | -283 |
| 2015 | R  | -160 | -425       | -429        | -354 | —    | —    | —    | —          | —    | -52  | -261 | -275 |
|      | M1 | -129 | -358       | -328        | -284 | —    | —    | —    | —          | —    | -72  | -215 | -243 |
|      | M2 | -129 | -355       | -339        | -308 | -171 | -240 | -114 | <b>-11</b> | -107 | -78  | -192 | -244 |
| 2016 | R  | -177 | -352       | -348        | -310 | —    | —    | —    | —          | —    | -129 | -151 | -307 |
|      | M1 | -129 | -272       | -255        | -264 | —    | —    | —    | —          | —    | -98  | -90  | -243 |
|      | M2 | -150 | -267       | -287        | -289 | -196 | -194 | -113 | -198       | -75  | -97  | -72  | -222 |



455 **Figure 1.** (a) The mean CMST sea ice drift and thickness averaged from September, 2010 to December, 2016. (b) The differences between CMST drift and NSIDC drift, the background color represents the magnitudes of ice velocity difference during the same period. The thick black line represents zonal and meridional sea ice gates to derive sea ice volume flux through the Fram Strait.



460 **Figure 2.** (a) The trajectories of 9 separate flights of HEM measurement campaigns carried out in the Fram Strait and the red dot denotes the site of ULS. Scatter plots of (b) daily mean sea ice thickness derived from CMST and HEM data, (c) monthly mean sea ice thickness derived from CMST and ULS data, (d) monthly average sea ice drift based on CMST and OSI SAF.



465 **Figure 3.** Seasonal variation of Arctic sea ice thickness. The thick black line represents the sea ice fluxgate in the Fram Strait used in this study.

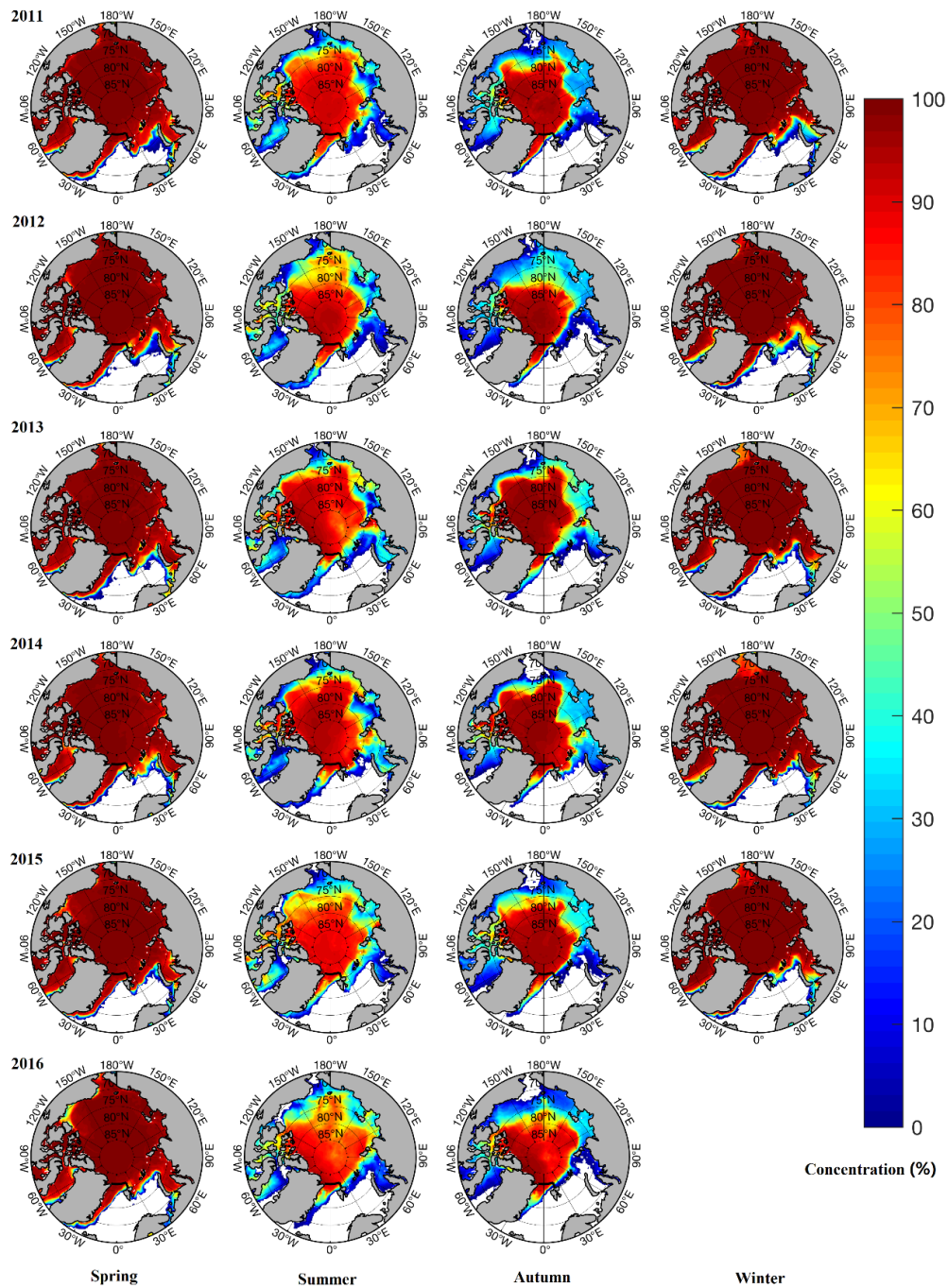
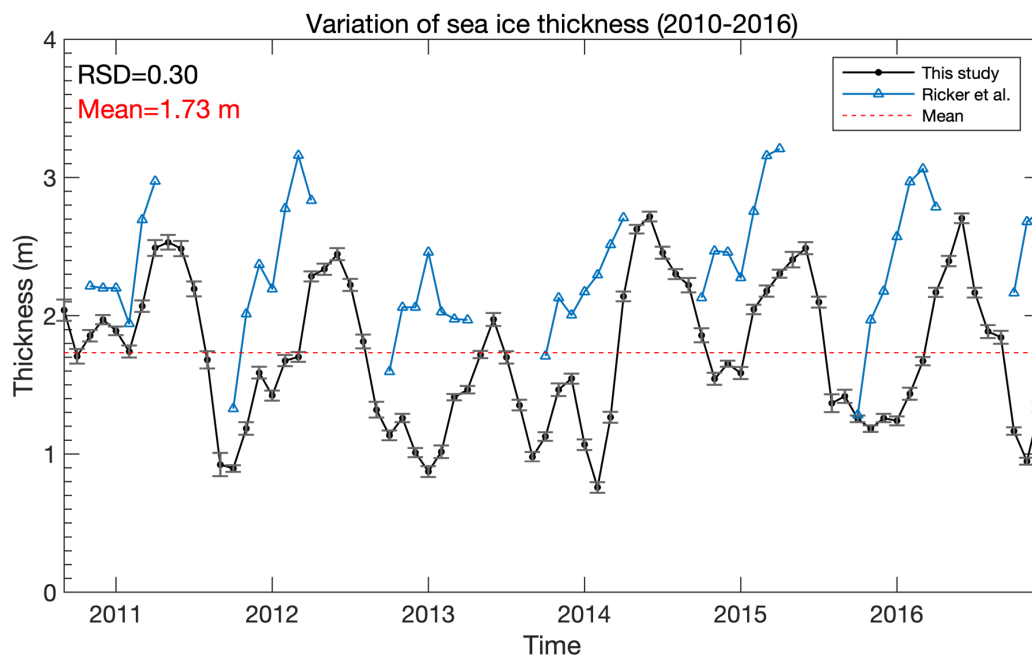


**Figure 4.** Seasonal variation of Arctic sea ice concentration. The thick black line represents the sea ice fluxgate in the Fram Strait.





470 **Figure 5.** CMST sea ice thickness averaged over the entire Fram Strait gate, from September 2010 to December 2016. The black dotted line denotes monthly mean ice thickness based on CMST data with corresponding standard deviations while the blue dotted line represents monthly mean ice thickness of CS2.

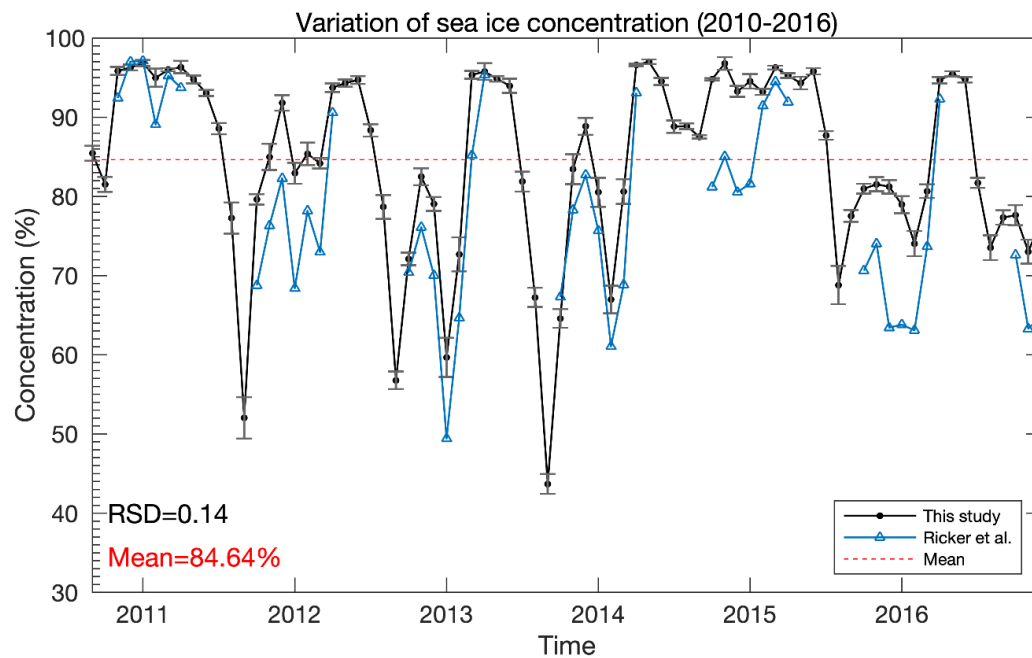






**Figure 6.** CMST sea ice concentration averaged over the entire Fram Strait gate, from September 2010 to December 2016. The black dotted line represents monthly mean ice concentration based on CMST data with corresponding standard deviations while the blue dotted line represents monthly mean ice concentration of OSI SAF.

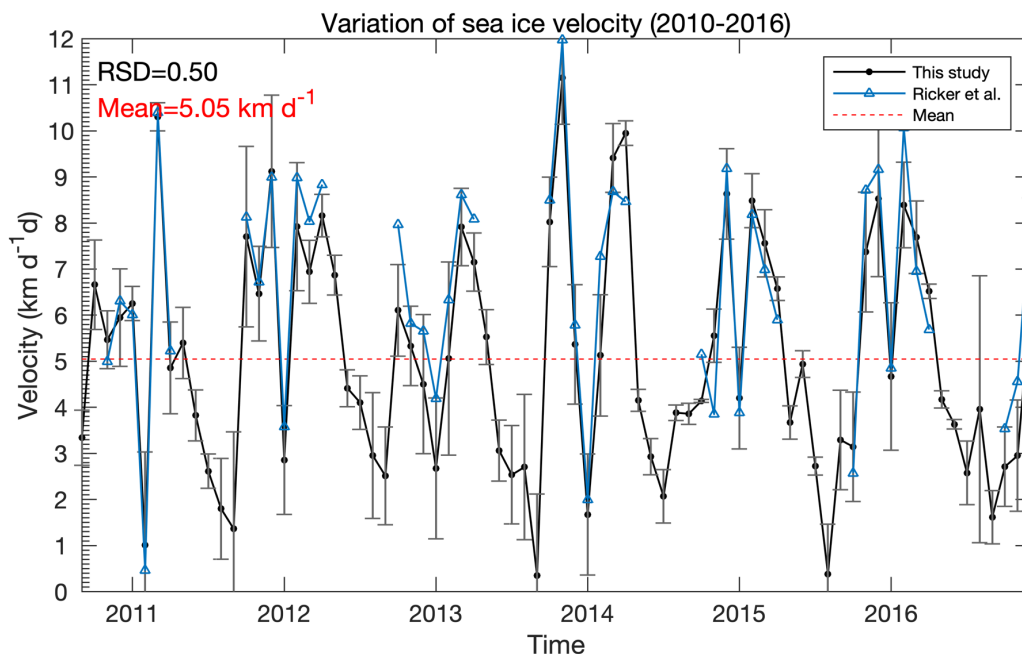


**Figure 7.** CMST sea ice drift averaged over the entire Fram Strait gate, from September 2010 to December 2016. The black dotted line represents monthly mean ice drift based on CMST data with corresponding standard deviations while the blue dotted line shows the monthly mean ice drift of OSI SAF.

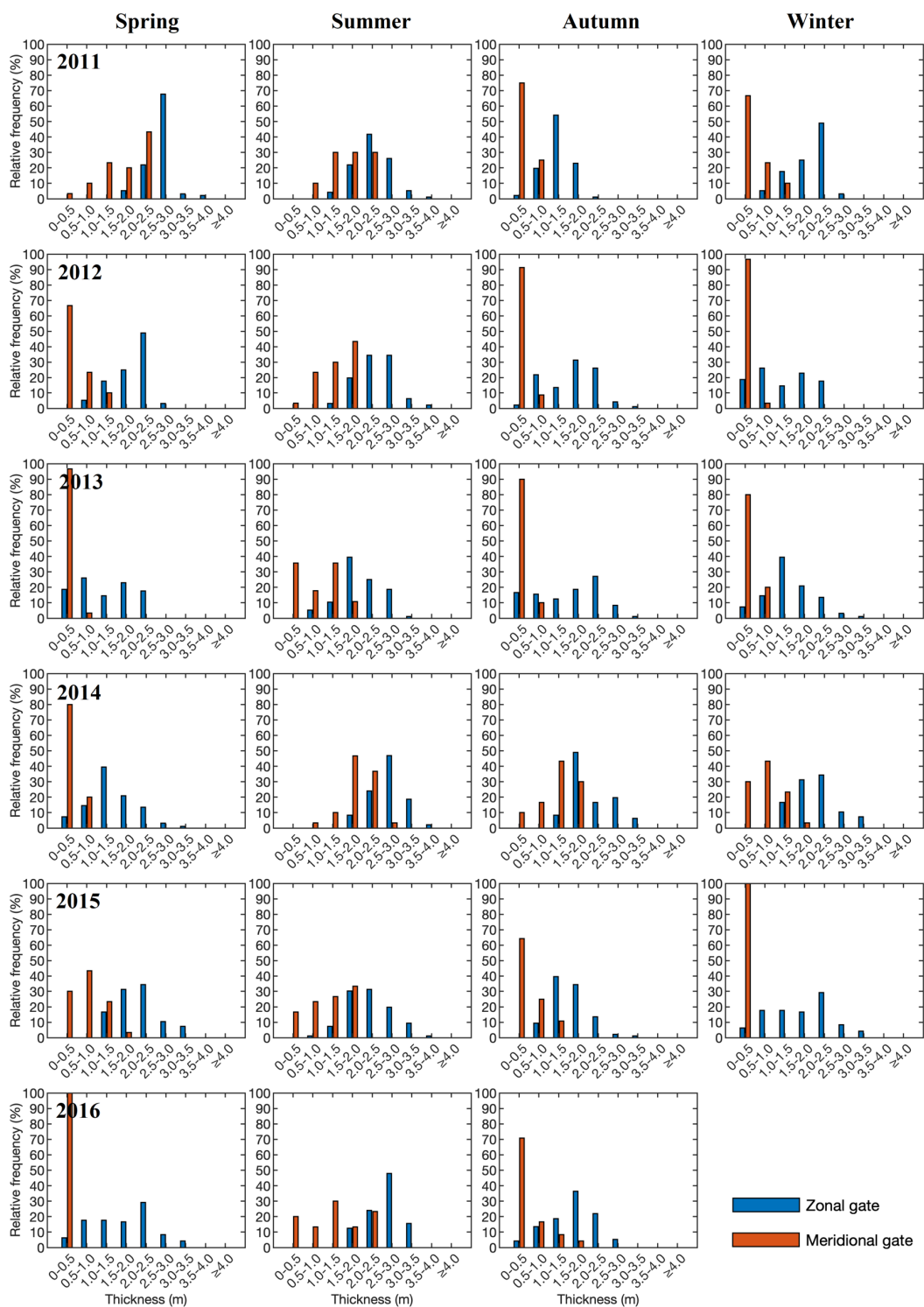
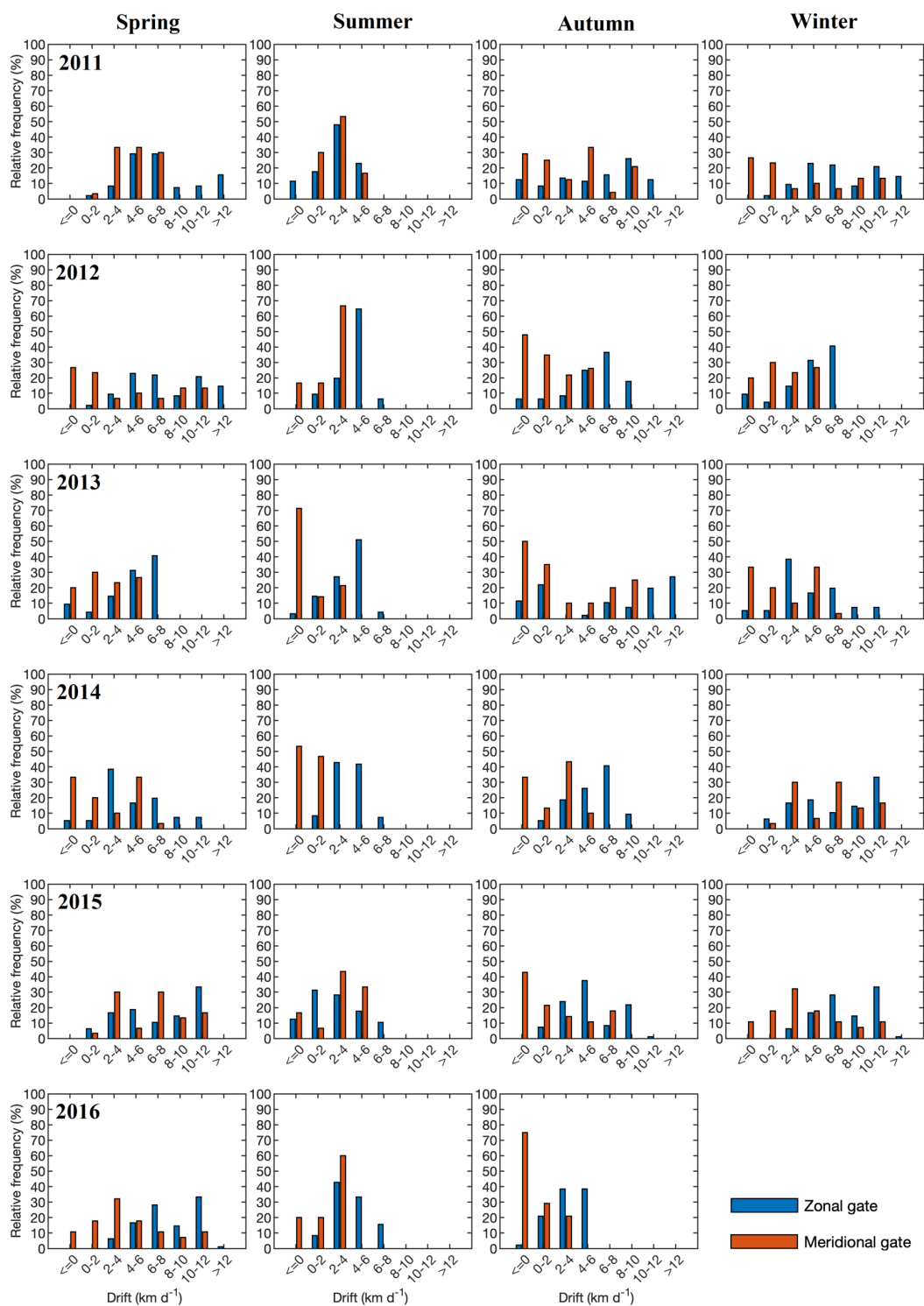


**Figure 8.** Seasonal variation of relative frequency of CMST sea ice thickness over the Fram Strait gate.



485 **Figure 9.** Seasonal variation of relative frequency of CMST sea ice drift over the entire Fram Strait gate.

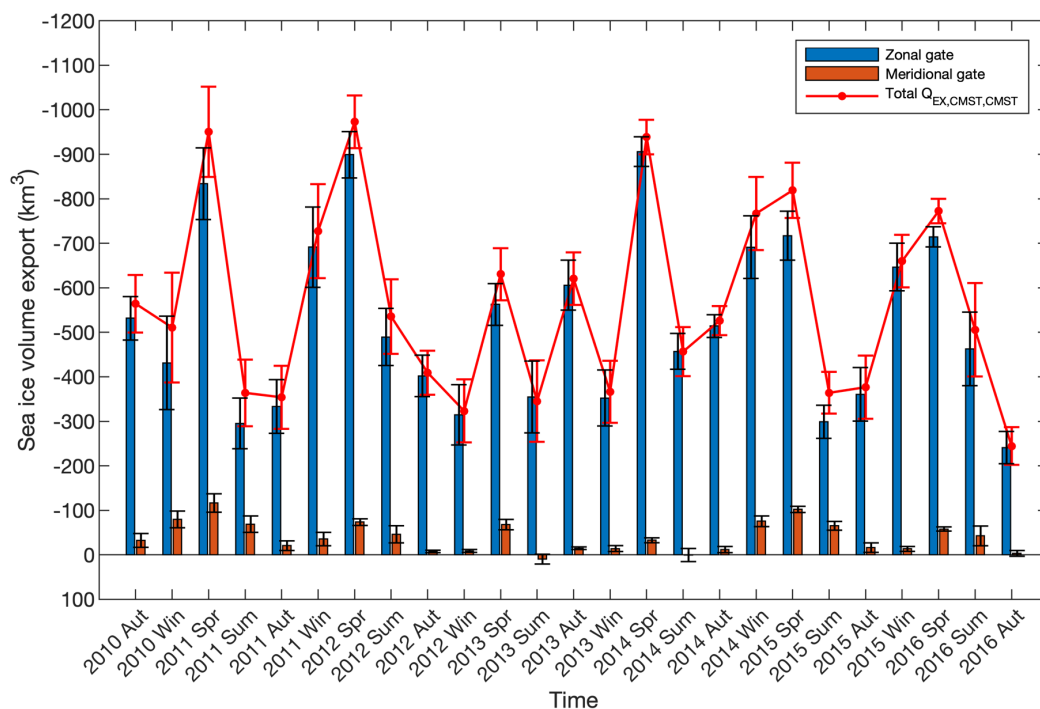
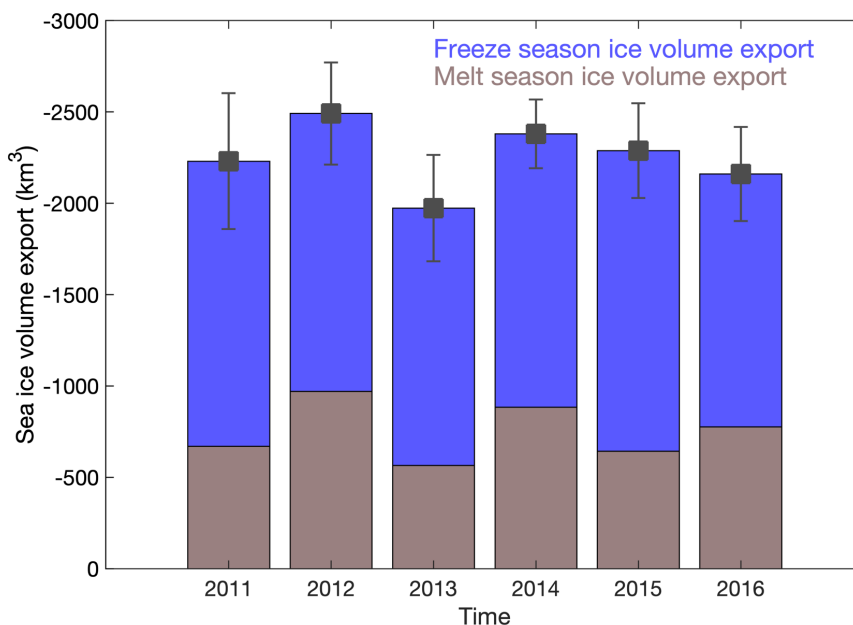


**Figure 10.** CMST seasonal Arctic sea ice volume export ( $\text{km}^3$ ) through the Fram Strait with corresponding uncertainty.



490 **Figure 11.** CMST interannual Arctic sea ice volume export ( $\text{km}^3$ ) through the entire Fram Strait with corresponding uncertainty.

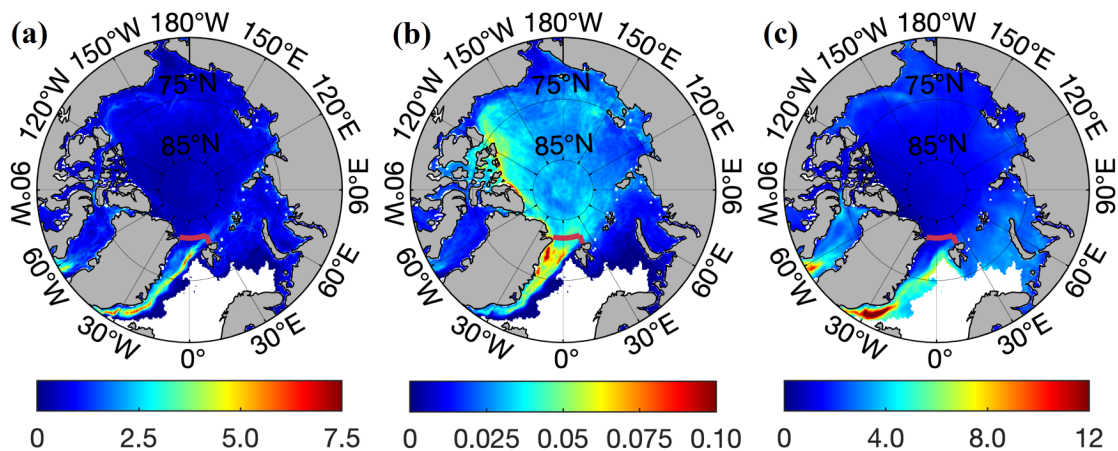


**Figure 12.** The mean ensemble standard deviation (SD) map of CMST (a) sea ice concentration (unit: %), (b) sea ice thickness (unit: m) and (c) sea ice drift (unit: km d<sup>-1</sup>) from September, 2010 to December, 2016. The thick red line represents zonal and meridional sea ice export gates to derive sea ice volume flux through the Fram Strait.

495